HHS Public Access

Author manuscript

Sci Transl Med. Author manuscript; available in PMC 2021 June 23.

Published in final edited form as:

Sci Transl Med. 2020 August 26; 12(558): . doi:10.1126/scitranslmed.abc0441.

Gastrointestinal synthetic epithelial linings

Junwei Li[1], **Thomas Wang**[1], **Ameya R. Kirtane**[1,2], **Yunhua Shi**[1,2], **Alexis Jones**[1], **Zaina Moussa**[1], **Aaron Lopes**[1], **Joy Collins**[1,2], **Siddartha M. Tamang**[1], **Kaitlyn Hess**[1], **Rameen Shakur**[1], **Paramesh Karandikar**[1], **Jung Seung Lee**[1], **Hen-Wei Huang**[1,2], **Alison Hayward**[1,2,3], **Giovanni Traverso**[1,2,4,*]

[1]Department of Chemical Engineering and David H. Koch Institute for Integrative Cancer Research, Massachusetts Institute of Technology, Cambridge, MA, 02139, USA.

[2]Division of Gastroenterology Brigham and Women's Hospital, Harvard Medical School, Boston, MA, 02115, USA.

[3]Division of Comparative Medicine, Massachusetts Institute of Technology, Cambridge, MA 02139, USA.

[4]Department of Mechanical Engineering, Massachusetts Institute of Technology, Cambridge, MA, 02139, USA.

Abstract

Epithelial tissues line the organs of the body, providing an initial protective barrier as well as a surface for nutrient and drug absorption. Here we identified enzymatic components present in the gastrointestinal epithelium that can serve as selective means for tissue-directed polymerization. We focused on the small intestine, given its role in drug and nutrient absorption, and identified catalase as an essential enzyme with the potential to catalyze polymerization and growth of synthetic biomaterial layers. We demonstrated that the polymerization of dopamine by catalase yields strong tissue adhesion. We characterized the mechanism and specificity of the polymerization in segments of the gastrointestinal tracts of pigs and humans ex vivo. Moreover, we demonstrated proof-of-concept for application of these gastrointestinal synthetic epithelial linings (GSELs) for drug delivery, enzymatic immobilization for digestive supplementation, and nutritional modulation through transient barrier formation in pigs. This catalase-based approach to in situ biomaterial generation may have broad indications for gastrointestinal applications.

[*]Corresponding author. cgt20@mit.edu, ctraverso@bwh.harvard.edu.

Author contributions: J.L. and G.T. conceived the idea and designed the project. J.L. and T.W. performed majority of the experiments, with help from A.R.K. for pharmacokinetic analysis, from Y.S. for real-time PCR quantification, from A.J. for western blotting, from Z.M. for oral toxicity study, from J.S.L. for cell fractionation, from H.-W.H. for mechanical stability analysis, from A.L. and K.H. for sample analysis using high-performance liquid chromatography and ultra-performance liquid chromatography–tandem mass spectrometry, from J.C., S.M.T., R.S. and A.H. for in vivo pig experiments. All authors were involved in data analysis. J.L., A.J., T.W., A.R.K. and G.T. wrote the paper with contributions from all authors.

Competing interests: G.T., J.L., T.W., Y.S., A.R.K. and Z.M. declare submission of provisional patent applications describing the materials and applications of gastrointestinal synthetic epithelial linings described here. Complete details of all relationships for profit and not for profit for G.T. can be found at the following link: https://www.dropbox.com/sh/szi7vnr4a2ajb56/AABs5N5i0q9AfT1IqIJAE-T5a?dl=0.

Data and materials availability: All data associated with this study are present in the paper and/or Supplementary Materials.

INTRODUCTION

The gastrointestinal (GI) epithelium serves as a protective layer against physical abrasion, chemical stress, and pathogens, as well as a site for sensing (feeding states), molecule transport of nutrients and drugs, and immunologic signaling(1, 2). Modulation of these activities has the capacity to aid in a broad array of treatments(3–9). Conversely, derangements of these functions are associated with disease(10–12). Given the distinct role of the GI epithelium and the specialized environment along the GI tract, progress has been made in epithelial targeting, including engineered tissue substitutes such as epithelial grafts, autologous cell-sheets, and plastic epithelium-sleeves as well as synthesized tissue adhesives (metal complexes, targeted nanoparticles, and small molecular superglues). These technologies are being investigated as potential tools for restoration of GI epithelial function and treatments of diseases such as type 2 diabetes, Crohn's disease, and mesenteric ischemia(3–7, 13–15). However, broad implementation of current tissue-targeting strategies has been limited due to multiple factors including invasive transplantation, potential immunogenicity, toxicity, and inconvenience, restricting selective small intestinal access(16–19). To address these limitations, enteric polymers with pH- and time-dependent dissolution properties including Eudragit L and FL and Eudragit S and FS have been widely used for targeted drug delivery in the small intestine and colon, respectively(20–23). The performance of enteric polymers is highly dependent on the GI pH and transit time under different fed conditions(24–26).

Here, we report the development of a GI synthetic epithelial lining (GSEL) system that uses an alternative mechanism for specific targeting and localization to the small intestine. Our approach was enabled by two design concepts: (i) development of tissue-specific catalyzed polymerization techniques for in situ growth of polymers on epithelial surfaces and (ii) identification and application of endogenous enzyme-dependent reactions to control the polymeric coating efficiency for specific anatomic targeting. We demonstrate this concept by combining catalase (CAT), an enzyme present in all aerobic organisms, with polydopamine (PDA), a mussel-inspired tissue adhesive(27, 28). In general, PDA polymerization is a slow process, with the reaction limited by low oxygen concentrations in normal dopamine oxidation conditions(27). We applied CAT-catalyzed decomposition of hydrogen peroxide, supplied at concentrations (0.066% by weight in the solution; 0.68–6.8 mg/kg in animals) recognized to be safe(29), and found that we could accelerate PDA polymerization by multiple orders of magnitude. As shown in Fig. 1A, the oral solution that we developed contains dopamine monomers and trace amount of hydrogen peroxide, which passes through the oral cavity, esophagus, and stomach to induce a GSEL coating on the small intestinal luminal surface. The hydrogen peroxide molecules diffuse freely between the small intestinal epithelium and the solution. The hydrogen peroxide diffuses into or is absorbed by intestinal epithelial cells and is rapidly broken down by intracellular CAT into oxygen, which is released out of the cells and mixed with extracellular monomers. These monomers near the epithelial surface are instantly oxidized into oligomers and further into polymers that crosslink with biomolecules exposed outside the epithelium(28), which contribute to a thin but strong PDA coating layer on the tissue. Unreacted monomers in the solution and unbound PDA are washed away from the epithelium. This type of tissue surface-initiated

polymeric coating may prevent potential bowel adhesions and obstructions, which are frequently induced by bulk crosslinking-based sealants or other conventional tissue adhesives(30). The catalytic PDA polymerization primarily occurs in the small intestine, due to higher expression of CAT in the small intestine relative to other parts of the GI tract including the esophagus, stomach and colon(31). Thus, small intestinal targeting with biomaterials is enabled by anatomic-specific distribution of natural enzymes along the digestive tract.

To evaluate the therapeutic value of the GSEL technology, we focused on three different clinical scenarios: intervention of lactose intolerance, regulation of intestinal glucose absorption, and improvement of administration efficiency for medications in pigs. We first investigated hypolactasia, low amounts or absence of lactase that causes lactose intolerance, as according to recent studies, about 70% of the world population has hypolactasia(32, 33). Restoring function of brush border enzymes in the small intestine, particularly β-galactosidase, could enable treatment of digestive disorders, improving patient prognosis and quality of life(34, 35). Another essential function of the small intestine is regulation of plasma glucose concentrations, which are frequently associated with metabolic disorders and systemic diseases, such as obesity, hyperinsulinemia, and diabetes mellitus(36). To modulate nutrient absorption in patients with these disorders, treatments such as gastric bypass surgery, intestinal sleeve placement, intestinal mucosal resurfacing, surgical adhesives, and GI electrical stimulation have been applied(5, 6, 8, 37, 38). However, these procedures can be invasive and manifest with adverse effects. The GSEL technology can offer a non-invasive, tissue-targeted method for regulating glucose (and nutrient) absorption. Moreover, the GSEL technology can prolong intestinal residence and enable sustained release of therapeutics in the small intestine. The development of oral sustained-release drugs is restricted by the rapid transit time of therapeutics in the GI tract. Attempts have been made to prolong the GI residence of drugs, especially in the small intestine, a more compatible environment for sensitive pharmaceuticals compared to the harsh acidity of the stomach, with little success(39, 40). Schistosomiasis, a major neglected tropical disease caused by parasitic worms, affects over 200 million people worldwide(41, 42). Praziquantel, with a half-life of 1–1.5 hours in humans, is the only anthelmintic drug frequently used to treat schistosomiasis, and is recommended to be taken orally 3 times per day. An alternate technology capable of prolonging intestinal retention to reduce dosing frequency could enhance medication adherence. We have therefore developed the GSEL technology to address these emerging clinical needs.

RESULTS

Endogenous enzyme-catalyzed PDA growth on epithelium

To demonstrate the acceleration of PDA polymerization by CAT in a hypoxic environment, mimicking the low partial pressure of oxygen in the GI tract, PDA polymerization rates were quantitatively evaluated in different reaction conditions in which dopamine was maintained at the same concentration (Fig. 1, B to D and fig. S1). In a hypoxic environment, the conventionally slow PDA polymerization was inhibited by 65% (fig. S1). The addition of a trace amount of hydrogen peroxide (H_2O_2), serving as a strong reducing agent, prevented

dopamine oxidation and almost quenched the reaction. As shown in Fig. 1C, the slow color change of the dopamine solution from clear to light gray over two hours indicates minimal PDA polymerization, and the clear dopamine-H_2O_2 solution indicates negligible PDA polymerization. In contrast, the dopamine solution with the addition of both CAT and H_2O_2 instantly turned to a dark brown color, demonstrating the accelerated PDA polymerization. In this study, the polymerized products catalyzed by CAT from both commercially purified enzymes and crude tissue lysates were confirmed to be PDA by both Fourier transform infrared (FTIR) and ultraviolet–visible (UV-Vis) spectroscopy (figs. S2 and S3). To further quantify the effect of CAT on PDA polymerization rate, a comparison of reaction kinetics was plotted by measuring the optical extinction of solutions at 700 nm (Fig. 1D), representing PDA formation(43, 44). The signal of the CAT-PDA combination rapidly increased and plateaued within 10 minutes. However, intensities of light extinction in other conditions were relatively low, even after 2 hours, of which the same intensity was reached within 20 seconds under CAT-catalyzed conditions, demonstrating an increase in the polymerization rate by about 400 times.

Next, we assessed whether endogenous CAT could expedite PDA polymerization and coating of the small intestine to achieve a GSEL. The porcine GI tract was chosen as the first model tissue, due to its anatomical and physiological similarities with the human digestive system(39, 45). Ex vivo tissues were incubated with the GSEL solution, containing dopamine as well as hydrogen peroxide at concentrations recognized as compatible with human ingestion(29). As shown in Fig. 1E, when the luminal surface of the small intestine was exposed to the GSEL solution, a dark-brown PDA coating was observed on the epithelial surface, demonstrating that PDA was formed in situ and deposited on anchor points of the tissue due to the high reactivity between PDA and primary amines in nearby biomolecules(28). In contrast, almost no PDA was observed on the serosal surface of the tissue. To further quantify the rate of PDA deposition, the amount of PDA coated on small intestine was analyzed kinetically. The coating kinetics showed rapid PDA signal development, reaching completion within 12 minutes (Fig. 1F), supporting rapid PDA coating formation. In addition to the efficiency, the specificity of GSEL was also evaluated by comparing the GSEL coating in different parts of the GI tract, including the esophagus, stomach, duodenum, jejunum, ileum, and colon. As shown in Fig. 1G, images of porcine tissue (6 mm in diameter) reveal apparent PDA coating on the duodenum and jejunum, relatively less PDA coating on ileum and colon, and negligible PDA coating on the stomach and esophagus. This coating pattern was additionally demonstrated through quantitative PDA signal analysis (Fig. 1H). The efficiency and specificity of GSEL supported further development of in vivo applications.

Mechanisms of GSEL formation at molecular, cellular, and tissue levels

To understand the mechanism of GSEL formation, we systematically investigated the GSEL coating process. We first evaluated whether endogenous CAT is the component that determines the catalytic PDA polymerization on epithelium. Porcine GI tracts were dissected and washed, the outer mucus layer was removed by aspiration, and then the rinsed tissues were homogenized to prepare tissue lysates, which were further diluted relative to the total protein concentration. These tissue lysates were added individually into the GSEL solution,

and the light extinction of each solution was measured after the reaction. As shown in Fig. 2A, signals of the PDA solutions with lysates of small intestinal epithelium were significantly higher relative to other lysates ($P < 0.05$). Additionally, similar trends were observed in a catalytic capacity analysis of these lysates through native gel electrophoresis and PDA staining (fig. S4). Only one sharp band can be visualized in each lane, supporting CAT's predicted role as the sole enzyme responsible for PDA polymerization. To further confirm the dominant role of CAT, small intestinal lysates were treated with either the CAT-specific inhibitor, to reduce CAT activity, or CAT antibody-coated magnetic beads, to deplete CAT through immunoprecipitation. The catalytic capacity of lysates decreased by about 80% after adding the inhibitor (Fig. 2B), and decreased by about 90% upon bead-mediated removal of CAT from samples (Fig. 2C), demonstrating that the GSEL process is CAT-dependent. Additionally, we confirmed that CAT present due to bacteria in the small intestinal mucus did not affect the GSEL coating process (figs. S5 and S6), showing that most of the H_2O_2 was not degraded or consumed in the intestinal lumen, and the amount of H_2O_2 was sufficient to activate oxygen release and PDA polymerization. In addition, we observed that the catalytic PDA polymerization primarily occurs in the small intestine, which is due to higher expression of CAT in the small intestine as compared to other segments of the GI tract. It has been previously shown that mRNA and protein expression of human CAT is higher in the small intestine as compared to other segments of the GI tract(31). We confirmed this through enzymatic activity evaluation (Fig. 2D), real-time polymerase chain reaction (PCR) quantification (Fig. 2E and figs. S7 and S8), and corresponding protein expression analysis (Fig. 2F).

Next, PDA epithelial deposition was characterized microscopically(46). Interestingly, through the GSEL coating process, PDA first deposits on the tips of the villi, followed by extension over the entire villus structure and surrounding area (fig. S9). Microscopic analysis showed a thin PDA layer tightly coated on the tips of the villi (Fig. 2G). PDA was confined to the luminal surface of the epithelium, demonstrating topical PDA polymerization with dopamine remaining on the luminal surface (figs. S10–12). Specific peroxisome/CAT staining studies showed that CAT is located inside peroxisomes, which have a high-density distribution in the villi but not in submucosa and other inner layers (Fig. 2H, left panels). Similar studies have confirmed that CAT 'particles' are present in peroxisomes of intestinal epithelial cells(47). To further confirm that peroxisomal CAT can catalyze PDA formation, dopamine was used for staining in place of the typical peroxisome/CAT substrate. As shown in Fig. 2H (right panel), dark-brown PDA spots were observed inside epithelial cells and the staining pattern was consistent with the conventional peroxisome/CAT staining, confirming the catalytic capacity of peroxisomal CAT towards PDA polymerization in sectioned tissue segments. The peroxisomal PDA pattern was not observed in GSEL-coated samples (Fig. 2G, left panels) which received GSEL luminally and were subsequently sectioned for microscopy without peroxisome/CAT staining.

Evaluation of GSEL-based tissue-coating performance in vivo

Having defined the mechanisms underlying GSEL formation, we next tested the in vivo performance of this tissue-coating technology in Yorkshire pigs. Under moderate anesthesia, the GSEL solution was directly administered to the small intestine or stomach through a

catheter under endoscopic visual guidance (Fig. 3A). Endoscopy was used to evaluate dynamics of GSEL in the small intestine (Fig. 3, B and C). A dark brown PDA layer was observed on the wall of the small intestine 20 minutes after administration, whereas no such PDA coating was visualized in the stomach (Fig. 3C and fig. S13). The GSEL solution remained stable in the stomach for 30–60 minutes (fig. S14), confirming the durability of the solution. To be noted, all animals were fasted overnight, and the gastric fluid was removed from the stomach before administration of the Tris-buffered GSEL solution (pH 8.5), thus minimizing the possible effect of pH on the stability of the GSEL solution and PDA polymerization(48, 49). Additionally, we did not observe any detectable increase of PDA and dopamine signal in the submucosa and blood after the GSEL coating by microscopy (fig. S10), UV-Vis spectroscopy (fig. S15), or liquid chromatography-tandem mass spectroscopy (fig. S16). Furthermore, no obvious increase of blood pressure or heart rate was detected in any animal throughout the procedures, demonstrating the lack of dopamine absorption and the supporting the early safety of the GSEL technology(50). The endoscopic video revealed that the PDA coating process contained three main steps. First, when the clear dopamine-H_2O_2 solution was first introduced to the small intestinal lumen, oxygen bubbles formed and the intestinal wall rapidly turned to a light yellow-brown color, indicating the rapid diffusion of hydrogen peroxide and initiation of PDA polymerization. Second, increasing amounts of oxygen bubbles were generated at the epithelium-solution interface (Fig. 3B) and released into the solution (Fig. 3C), confirming the rapid decomposition of hydrogen peroxide and providing evidence for the mechanism of oxygen release. Third, the interfacial oxygen catalyzed PDA polymerization and adhesion to intestinal epithelium, whereas the GSEL solution remained in a liquid state and the intestinal lumen remained expanded, alleviating concerns about bowel adhesion and obstruction. Our results show that, after coating, the solution inside the lumen also turned a dark brown color, likely due to the diffusion of unbound PDA into the solution.

To directly evaluate coating formation, a laparotomy was performed on a pig. A non-crushing clamp was applied at the small intestine before endoscopic administration of the GSEL solution into the intestine, as shown in Fig. 3D. The GSEL solution filled the intestinal cavity to the clamp site, unable to pass distally to the lower small intestine. The tissue adjacent to the clamp was isolated, washed, and opened. Compared to the control segment (distal to the clamp), the tissue exposed to the GSEL solution showed enhanced PDA coating density, confirming the tissue-coating performance of GSEL in vivo.

Next, we investigated whether the GSEL technology could enable safe and prolonged intestinal retention of the PDA coating, a key feature for future applications. PDA shedding from epithelium was endoscopically visualized 24 hours after application, indicating that the coating is transient. To further evaluate the kinetics of GSEL retention radiographically, we first modified conventional X-ray contrast agents by encapsulating radio-opaque particles in PDA (fig. S17A). These PDA probes were suspended in the GSEL solution and thereby incorporated into the PDA coating layer, which was enabled by the chemical crosslinking between reactive PDA on the probe surface and dopamine monomers or oligomers in the GSEL solution (Fig. 3E)(28). This co-coating performance was first characterized through ex vivo studies (fig. S17, B and C), in which tissue coated with PDA probes were visualized radiographically, and no signal decay was observed after rinsing the epithelial surface with

water, demonstrating the stability of the PDA-probe coating. When the PDA probe-suspended GSEL solution was administered to healthy pigs, X-ray signal enhancement was observed in the small intestine (Fig. 3F and fig. S18A). However, when an equal concentration of conventional contrast agent was administered to the pigs, the resulting small intestine X-ray signal was weak in comparison. It is also worth noting that, after rinsing the imaged area, signal of conventional probe was barely detectable whereas PDA probes were still visualized (Fig. 3F), with an 8.9-fold higher signal intensity (Fig. 3H), demonstrating the efficient incorporation of PDA probes and the stable coating of PDA on the tissue.

To monitor the intestinal retention of PDA over time, a series of X-ray images of the same anatomic location were taken periodically (Fig. 3G and fig. S18B). Animals consistently consumed a liquid diet during imaging, mimicking realistic conditions and testing the stability of the PDA coating in the presence of food. A quantitative signal intensity analysis was performed on the small intestine and surrounding tissues (Fig. 3I). When conventional probes were administered to the pigs, the contrast signal from the X-ray images in the small intestine was reduced by 2 hours, likely due to the relatively weak tissue adhesion. However, when PDA probes were administered, a distinct contrast signal was observed in the small intestine after food exposure for 2 hours, decreasing by 28% at the sixth hour, showing the prolonged intestinal retention of the PDA coating. The PDA signal reduction is likely due to the fast renewal of the intestinal mucus through goblet cell secretion which occurs within ~12–24 hours and frequent turnover of epithelial cells through stem cell proliferation (~1–5 day)(51). The polymeric coating layer, as well as epithelium underneath the PDA, is shed into the lumen of the intestine. Notably, the intestinal signal dropped to the pre-administration intensity after 24 hours, indicating complete elimination and transient residence of the PDA coating layer. This confirmation of the transient properties of the PDA coating supports the potential safety of the GSEL technology.

GSEL for regulation of enzymatic digestion, nutrient absorption, and drug release

To demonstrate the versatility of the GSEL technology, we evaluated the therapeutic value of the technology in three different scenarios (Fig. 4A). PDA is highly reactive with many chemical groups, such as amine, phenol, and sulfhydryl groups, enabling the facile incorporation of functional agents into the PDA coating layer(28). Three types of functional agents were incorporated into the GSEL system: digestive enzymes, a nutrient blocker, and an anthelmintic drug. First, the GSEL technology was used to improve digestion efficiency by incorporating digestive enzymes into the PDA coating layer on small intestinal epithelium (Fig. 4B). If the GSEL technology can be used to coat exogenous β-galactosidase on intestinal epithelium, it would augment the digestion of lactose in the small intestine. To demonstrate the ability of the GSEL technology to improve lactose digestion, the GSEL solution with suspended β-galactosidase was used to coat the small intestine of a sedated pig, using a laparotomy to provide access to the small intestinal mucosa. The β-galactosidase activity of the coated epithelium was then evaluated after rinsing the tissue. The coating efficiency was confirmed through the analysis of β-galactosidase activity with and without the key agents (β-galactosidase and GSEL solution). As shown in Fig. 4C, quantitative comparison of β-galactosidase activity indicated an about 20-fold increase in

digestion efficiency upon the addition of the GSEL-based β-galactosidase coating to the porcine small intestine. In contrast, no obvious enhancements of β-galactosidase activity were detected in control groups (without β-galactosidase, without GSEL solution, or without both), confirming that the β-galactosidase activity increase was due to its pairing with the GSEL technology. Additionally, when only the GSEL solution was administered, no obvious reduction of digestive enzyme activity was observed compared to uncoated tissues. This consistent baseline enzymatic activity indicates that neither the coating chemistry (the crosslinking between PDA and epithetical biomolecules) nor the coated PDA itself inhibited the intrinsic digestive enzyme activity of epithelium, demonstrating the permeability of the PDA coating in the small intestine to allow molecules to pass through by diffusion. The GSEL technology opens an avenue to augment and supplement digestive functions in the small intestine and a promising mechanism to treat digestive disorders.

Next, we aimed to develop a transient impermeable barrier to regulate nutrient absorption. We demonstrated the ability of the GSEL technology to modulate nutrient exposure, especially glucose absorption, in the small intestine. To provide a barrier to prevent glucose uptake, we coated the small intestinal epithelium with an impermeable PDA coating (Fig. 4D). Nano-crosslinkers (PDA nanoparticles) were added to the GSEL solution to produce a highly crosslinked PDA coating layer with ultralow permeability. As shown in fig. S19, the additional nano-crosslinkers are about 527 nm in diameter with a uniform size distribution. These hydrophilic nano-crosslinkers suspended in the GSEL solution were thereby incorporated into the PDA coating layer, which was enabled by the chemical crosslinking between reactive catechol and amine groups exposed on the surface of nano-crosslinkers and dopamine monomers or oligomers in the GSEL solution. Thus, the incorporation of crosslinkers increases the number of covalent bonds inside the PDA coating, enabling a highly compact PDA coating layer with low permeability(52, 53). To validate the nutrient-regulating function, GSEL solution with suspended nano-crosslinkers was endoscopically administered to pigs. After GSEL coating, oral glucose was endoscopically administered to the pigs, followed by a standard oral glucose tolerance test (OGTT). Blood glucose concentrations were monitored to quantify the intestinal glucose absorption. As shown in Fig. 4E, control pigs, without the GSEL coating, had blood glucose concentrations increase dramatically after oral glucose administration. However, animals treated with the GSEL solution showed reduced blood glucose responses. Quantitative comparison of blood glucose concentrations from pigs with and without the GSEL coating showed an average of 73.3% reduction of glucose concentrations in the GSEL-treated animals over controls, representing six individual experiments on six different pigs. This reduction in glucose response demonstrated the ability of the GSEL technology to effectively reduce postprandial glucose absorption. Additionally, the GSEL barrier showed efficient blocking abilities of different nutrients, and the blocking efficiency could be modulated by tuning the crosslinking density of the GSEL coating layer (fig. S20). Furthermore, we confirmed that the glucose absorption barrier is transient, with normal glucose absorption being restored after 24 hours (fig. S21). These results address the clinical need of non-invasively blocking glucose absorption in the small intestine, supporting the feasibility of GSEL technology as a potential therapeutic approach for patients with type 2 diabetes mellitus.

Next, we investigated the GSEL technology as a system for oral drug delivery, demonstrating its ability for sustained release of therapeutics in the small intestine. Praziquantel was chosen as the model drug to test the ability of GSEL technology to prolong intestinal residence. As shown in Fig. 4F, praziquantel particles (powder) were encapsulated in PDA to incorporate the drug into the PDA coating layer. Pharmacokinetics studies were carried out using a single oral administration of the praziquantel-GSEL solution in pigs to investigate the release kinetics. After administration, blood samples were collected and analyzed by liquid chromatography-tandem mass spectroscopy for serum praziquantel concentration. Quantitative comparison of the pharmacokinetics revealed that the retention time of the praziquantel when delivered with the GSEL solution was significantly extended relative to the conventionally administration (Fig. 4G). When the praziquantel control (without the GSEL solution) was administered conventionally, the drug was rapidly cleared from blood, and no drug was detected at or after 24 hours. However, blood concentrations of praziquantel administered through the GSEL technology sustained for more than 6 hours, with an average concentration of 20.0 ng/ml still detectable at 24 hours, higher than the average control drug concentrations (15.1 ng/ml) at 6 hours. Quantitative analysis of pharmacokinetic parameters, including area under the curve (AUC) and half-life, was conducted using a non-compartment pharmacokinetics model. Results from 3 large-animals showed a 4-fold increase between the AUC values of the praziquantel with the GSEL solution (905.8 ng h/ml) and praziquantel control (222.4 ng h/ml). Additionally, the half-life of praziquantel increased by 10-fold (from 1.3 hours to 13 hours) when administered using the GSEL technology, demonstrating the prolonged intestinal residence of the drug. Notably, praziquantel is primarily metabolized by cytochrome P450 enzymes, specially CYP3A4 present in the small intestine and liver(42, 54). To confirm that the GSEL coating did not affect the drug metabolism, the CYP3A4 activity of epithelium with and without the PDA coating layer were measured and compared (fig. S22), and no change in CYP3A4 activity was observed after the GSEL coating. The sustained-release of praziquantel through the GSEL technology expands the effectiveness of treatment options for schistosomiasis, and is also applicable to diseases for which regimented adherence is essential for efficacy.

Ultrafast and stable coating of human tissue using GSEL

The GSEL technology is designed to be applicable to human tissues and suitable for clinical translation. Fresh resected tissue specimens from human small intestine were coated to test for compatibility with the GSEL technology. Similar to porcine tissue-coating results, PDA coating was apparent on the human small intestinal surface (Fig. 5A). However, PDA signals developed more rapidly in human tissues compared to porcine tissues, with coating completion time decreasing from 12 to 3 minutes (Fig. 5B), likely due to higher expression of CAT in the human small intestine. The relationship between small intestinal CAT activity and GSEL coating density was analyzed using human, porcine, and murine tissue specimens, demonstrating an association between GSEL coating density and enzymatic activity (fig. S23). The human and porcine small intestines exhibited 60% more PDA development compared to the murine small intestine, due to their strong enzymatic activity. To further demonstrate the robustness of the GSEL technology for human tissue coating, tissue specimens from 3 deceased donors were tested with the PDA coating. Additionally, five assessments were performed on random sites of the small intestine (from donors of

different age, race, and gender) to confirm consistent PDA coating performance. The human and porcine GI tracts exhibit similar GSEL coating patterns (fig. S24), due to higher expression of CAT in the small intestine of both species as compared to other segments of the GI tract(31). As shown in Fig. 5C, images of tissue (6 mm in diameter) revealed highly consistent PDA coating with obvious signal enhancement. These tissue specimens, coated through the GSEL technology, were further examined microscopically. Consistent with the porcine results, microscopic and histological analyses of frozen and formalin-fixed paraffin-embedded (FFPE) human tissue specimens showed a thin layer of the PDA coating on the exterior villi of the small intestine (Fig. 5D). After exposure to the GSEL solution, the epithelial layers remained intact, with staining patterns similar to the unexposed controls, demonstrating the absence of tissue toxicity.

To further evaluate the biocompatibility of the GSEL technology, we characterized the cytotoxicity of PDA on multiple cell lines: HeLa, COLO320DM, Caco-2, Hep3B, and HS 895.T (fig. S25). No obvious cytotoxicity was observed after 6–48 hour in vitro incubation. Furthermore, we systematically assessed the oral toxicity of the GSEL solution by following guidelines issued by the Organization for Economic Co-operation and Development (OECD) with minor modifications. Specifically, rats were exposed to the GSEL solution over a period of 4 weeks, based on a repeated dose 28-day toxicity study method recommended by Good Laboratory Practice (GLP)(55). During the 28-day exposure period, no obvious differences in body weights were observed between rats exposed to the GSEL solution and controls (fig. S26). Additional hematological measurements, blood biochemistry tests (tables S1 and S2), and histopathological examinations further confirmed the absence of oral toxicity (fig. S27), supporting the favorable biocompatibility of the GSEL technology, indicative of a minimal risk for forthcoming preclinical and clinical trials.

Human tissue-coating stability is a critical factor for clinical translation of the GSEL technology. The small intestine provides a dynamic environment, where physical forces (peristalsis and segmentation) and chemical exposures (chyme, gastric acid and intestinal fluid) have potential to damage the PDA coating (fig. S28). The stability of the tissue coating was evaluated in a series of physical and chemical conditions. As shown in Fig. 5E, no obvious PDA signal reduction was observed under mechanical stirring and scratching (movies S1 and S2). Quantitative signal intensity analysis showed that about 80% of the PDA coating remained strongly attached after vigorous scratching of the small intestine using the spine of a scalpel (Fig. 5F). In addition, the stability of the PDA coating was further confirmed by incubating PDA-coated human tissue in different solutions for 24 hours. The PDA coating layer was highly stable in simulated intestinal and gastric fluid, and other extreme conditions (ethanol and concentrated saline) (Fig. 5G). These results support the stability of the GSEL coating technology in the human small intestine and help establish feasibility for future human studies.

DISCUSSION

The small intestine is a versatile organ with multiple physiologic functions. Intestinal epithelium is not only a key protective barrier, but also an essential site of absorption. The potential of intervention in the small intestine for digestive disorders and systemic disease

treatments has intrigued and motivated scientists to develop a variety of targeted medications(1, 2, 5–7). However, the challenge of small intestine-specific targeting has limited broad adoption(17, 18). A simple and versatile strategy to allow selective small intestinal targeting could expand our capacity to treat a broad range of conditions. Here we report the GSEL technology that enables targeted therapeutic deposition and intervention in the small intestine. The GSEL technology is based on two concepts: (i) design of a polymerization system catalyzed by the epithelial enzyme, and (ii) control of polymeric coating efficiency through enzymatic activity for specific tissue-targeting. We have identified an endogenous CAT-accelerated polymerization reaction that allows rapid PDA coating on the small intestinal epithelium without deposition on other sites of the GI tract. Inspired by the cellular anti-oxidation response(56), we found that CAT in small intestinal epithelial cells enables oxygen release and accelerates PDA polymerization (~400 fold increase). More importantly, the in situ-generated PDA rapidly crosslinks with nearby biomolecules exposed outside epithelium and therapeutic agents suspended in solution, forming a thin but strong coating with versatile functions on the small intestine. The GSEL technology spontaneously achieves this specific small bowel coating due to high epithelial CAT activity of small intestine relative to other parts of the digestive tract.

To further understand the biological mechanisms of GSEL in detail, a series of investigations were performed at molecular, cellular, and tissue levels, consistently confirming the dominant role of CAT in tissue coating and targeting with GSEL. Recognizing the detailed principles of GSEL, we envision that this tissue-accelerated polymerization reaction may also evolve or augment functions of a wide variety of organs due to the broad yet diverse distribution of CAT in the human body. In this study, we evaluated the GSEL technology in the GI tract in a large animal model. The in vivo GSEL coating performance has been studied through various techniques, including endoscopic examination, intestinal ligation, and X-ray imaging, which consistently showed the robustness of the GSEL technology, demonstrating key features (prolonged but transient intestinal residence) of the coating layer. Additionally, no clinical, endoscopic, or radiographic evidence of GI perforation, inflammation, or obstruction was observed over multiple experiments. The biocompatibility of GSEL was carefully characterized by following OECD guidelines and confirmed the absence of oral toxicity.

The flexibility of this technology has allowed us to go beyond technological development and proceed to evaluate its therapeutic value in several clinical scenarios in pigs. We applied GSEL to address lactose intolerance by coating digestive enzymes on the small intestinal epithelium. The results show that β-galactosidase coated on the tissue improves the digestion efficiency of lactose by about 20 times, demonstrating our capacity to augment or supplement enzymatic-mediated intestinal digestion. Furthermore, the GSEL technology was assessed in the regulation of intestinal glucose absorption, an urgent need for patients suffering from type 2 diabetes mellitus. A poorly permeable coating layer, serving as a glucose-blocking barrier, was developed to minimize postprandial glucose absorption (~70% reduction of glucose responses). We also expanded the application of GSEL to improve administration efficiency for medications with inconvenient regimens, demonstrating its capability for sustained release of therapeutics. The GSEL-based method for administration of praziquantel (an anthelmintic drug) achieved long-lasting (over 24 hours) drug

concentrations in systemic circulation (10-fold increase of half-time value), suggesting the potential to improve medication dosing options for patients with schistosomiasis and other frequently dosed treatments.

For the potential human application, several challenges need to be addressed. Further preclinical safety studies will be needed in other large animal models such as dogs and nonhuman primates, which will help inform further development and successful translation of the GSEL platform in specific dosage forms (capsule, pill or gel containing alternative monomers) for human trials. Regular nutritional evaluation, monitoring, and supplementation would be required for future human studies(57). Additionally, the GSEL solution was administrated to the animals through a catheter under endoscopic visual guidance(39, 40), enabling consistent delivery of the solution to the small intestine or stomach. Although the GSEL solution is expected to quickly pass through the oral cavity and further into esophagus within seconds(26), the stability of the solution in the oral cavity was not studied here. Regardless, the degradation of H_2O_2 in the oral cavity may still affect the stability of the GSEL solution and consistency of therapeutic effects. Thus, understanding the degradation kinetics of H_2O_2 in the oral cavity, and the resulting effect on GSEL solution stability, requires further evaluation. In addition, strategies to prevent the degradation of H_2O_2 [for example, through the use of drinking straws and GSEL capsules (fig. S29)] also requires further assessment.

We envision broad technology adoption and application of the GSEL technology. For wide implementation, a range of therapeutic molecules would be incorporated into the GSEL system, and their formulations will need to be optimized for efficacious treatment. Additional clinical studies will be needed to test therapeutic efficacies of these dosage forms. The GSEL system has potential as a platform technology for management and treatment of various diseases.

MATERIALS AND METHODS

Study design.

The GSEL technology was developed with the goal of enabling targeted therapeutic deposition and intervention in the small intestine. This objective was addressed by (i) identifying CAT present in the small intestine as an essential enzyme with the potential to catalyze polymerization and growth of PDA on intestinal epithelium and (ii) demonstrating the potential application of these synthetic epithelial linings for drug delivery, enzymatic immobilization for digestive supplementation, and nutritional modulation through transient barrier formation. The mechanism and specificity of the GSEL was characterized ex vivo in segments of the GI tracts of pigs and humans. The in vivo GSEL coating performance was evaluated in the GI tract in a large animal (pig) model through multiple techniques including endoscopic examination, intestinal ligation, and X-ray imaging. Yorkshire pigs (45–75 kg) were chosen as the model, given their anatomic and genomic similarities to the human digestive system. We first applied GSEL to address lactose intolerance by coating β-galactosidase on the small intestinal epithelium and tested the ability of GSEL to improve lactose digestion. Next, we applied GSEL to modulate glucose absorption in the small intestine by coating a transient impermeable barrier on the small intestinal epithelium, and

tested the ability of GSEL to minimize postprandial glucose absorption. Additionally, we applied GSEL to prolong the GI residence of drugs by coating praziquantel on the small intestinal epithelium, and tested the ability of GSEL for sustained release of therapeutics. The biocompatibility of GSEL was characterized according to OECD guidelines. All animal experiments were approved by and performed in accordance with the Committee on Animal Care at Massachusetts Institute of Technology(39, 40). Group and sample size for each experiment are indicated in each figure legend. The sample sizes, determined before study initiation, were guided by prior proof-of-concept studies in the area of GI drug delivery and electronics(39, 58, 59). Independent experiments for each sample were performed on different animals. All rats were randomly divided into different experimental groups, but there was no pre-established randomization plan for in vivo pig studies, because pigs were only available on demand.

GSEL solution preparation.

Dopamine hydrochloride powder (500 mg) was dissolved rapidly in Tris buffer (50 mM, 50 ml) at pH 8.5, followed by quick addition of H_2O_2 (1M, 1ml). The mixed Tris-buffered GSEL solution was used fresh before administration. Solid urea H_2O_2 (as a replacement of H_2O_2 solution) was used to prepare the GSEL capsules (size 000), which were filled with dopamine hydrochloride, Tris base and urea H_2O_2 powders. The sources of chemicals and materials are provided in the Supplementary Materials.

In vitro evaluation of CAT catalyzed PDA polymerization.

GSEL solutions (200 μl) were prepared first and added into 96-well plates, followed by addition of CAT [1 mg/ml, 5 μl in 1X phosphate-buffered saline (PBS) buffer]. All solutions were placed in containers (BD GasPak EZ) with a low partial pressure of oxygen. The reaction mixture was maintained at 37 °C for 10–130 minutes. Extinction of solutions at 700 nm was measured using a plate reader (Tecan). The results were compared with those obtained from solutions without addition of CAT and H_2O_2, and those obtained from reactions in conventional conditions (in the air).

PDA characterization using FTIR and UV-Vis spectroscopy.

PDA standard was prepared by polymerization of the dopamine solution (10 mg/ml) in the conventional condition (in the air) for 24 hours(27). For CAT catalyzed PDA, CAT (1 mg/ml) was placed in a dialysis device (5 ml), which was merged into the GSEL solution (100 ml) for 24 hours. After reaction, the PDA solutions were measured by FTIR (Nicolet) and UV-Vis spectroscopy (Varian Cary 100).

Ex vivo evaluation of the GSEL coating performance.

Porcine tissues were acquired from the Blood Farm Slaughterhouse (West Groton, USA). Pigs were euthanized, and fresh tissue was resected and stored on ice. Human tissue specimens were acquired from 4 donors (National Disease Research Interchange, NDRI, USA) with different age, race, and gender. Tissues (12 cm^2) were exposed to the GSEL solution (10 ml) and washed with PBS buffer (1X) 3 times to remove excess PDA. Samples (6 mm in diameter) were collected at 3–5 random sites of PDA coated tissue, and images of

the samples were analyzed for quantification of the PDA coating. ImageJ was used to identify regions of interest that included PDA coated tissues and excluded 'blank' tissue-free areas. Identical analysis was performed on all samples in each group to obtain an overall average PDA signal intensity and assess signal variation. Tissues were exposed to the antibiotic-antimycotic solution (10X, Gibco) and washed with PBS buffer (1X) 3 times to remove bacteria in mucus. Villi was stripped off from the luminal surface of small intestinal tissue (opened lengthwise) placed on the ice-cold substrate. Cell fractionation was performed on villi by using cytoplasmic and membrane extraction kits (NE-PER, Mem-PER) based on the protocol from kits. The CYP3A4 activity was measured by using the CYP3A4 activity assay (Abcam) based on the assay protocol.

Evaluation of CAT expression in tissues.

Fresh porcine tissues were collected for real-time PCR and western blotting. Total RNA was isolated and reverse transcribed into cDNA with standard protocol. The mRNA expression was measured using LightCycler 480 II system (Roche). CAT mRNA expression was normalized to housekeeping genes (β-actin, 18S, GUS, and GAPDH) and expressed as the percentage of negative control. For western blotting, tissue lysates were resolved on SDS-PAGE gel with standard protocol. Anti-CAT [1:500 diluted in Tris-buffered saline with TritonX 100 (TBST) buffer] and anti-β-actin (1:1000 diluted in TBST buffer) were used as primary antibodies. Secondary antibodies (1:2000 diluted diluted in TBST buffer) were used for specific detection. CAT signals were developed using SuperSignal West Femto Maximum Sensitivity substrate, and β-actin signals were developed using Pierce ECL western blotting substrate. The western blots were imaged on ChemiDoc XRS+ system (Bio-Rad) and analyzed with Image Lab 3.0.

Microscopic analysis of PDA coated tissues.

PDA coated small intestines were snap-frozen and embedded in optimal cutting temperature (OCT) compound. The fixed tissues were cut into 40-μm-thick sections with a cryostat (Leica Biosystems). Specific peroxisome/CAT staining was performed as previously reported(47). The uncoated tissue sections were stained with the 3,3'-diaminobenzidine (DAB) substrate or GSEL solution (1 ml) for 10 minutes. The slides were scanned by Aperio digital pathology slide scanner (Leica Biosystems) and analyzed with Aperio ImageScope (Leica Biosystems).

In vivo evaluation of the GSEL coating performance.

All animal experiments were approved by and performed in accordance with the Committee on Animal Care at Massachusetts Institute of Technology. A large animal model, 45–75 kg Yorkshire pigs (Tufts University, Grafton, MA, USA), was chosen to test the in vivo performance of the GSEL coating. Pigs were fed daily in the morning and in the evening with a diet consisting of pellets (laboratory mini-pig grower diet 5081), in addition to a midday snack consisting of various fruits and vegetables. The pellets consisted of ground oats, alfalfa meal, wheat middlings, soybean meal, dried beet pulp, salts, and other micronutrient supplements. Before oral administration, the pigs were sedated with Telazol (tiletamine/zolazepam) (5 mg/kg IM), xylazine (2 mg/kg IM), and atropine (0.05 mg/kg IM), intubated, and maintained with isoflurane (1 to 3% through inhalation). Also, the gastric

fluid was removed from the stomach before administration of the Tris-buffered GSEL solution (pH 8.5). The GSEL solution (1 ml/kg) was orally administered to the intestine or stomach via a catheter under endoscopic visual guidance. Gastrointestinal endoscopy videography was used for real-time recording of PDA formation after delivery of the GSEL solution, and the endoscopic camera was placed both inside and outside the GSEL solution. To directly evaluate the PDA coating, a laparotomy was performed on pigs. A non-crushing clamp was applied at the small intestine before administration of the GSEL solution into the intestine. GSEL solution filled the intestinal cavity up until the clamp site, unable to pass down to the lower small intestine. After 20 minutes of administration, pigs were euthanized and the tissue nearby the clamp was isolated, washed, and opened up. All animals were euthanized prior to tissue harvest. Macroscopic images of tissues were taken to evaluate the PDA coating performance. Blood pressure and heart rate of pigs were monitored during the procedures by using the Cardell Touch multi-parameter monitor (Midmark). Additionally, no clinical or endoscopic evidence of gastrointestinal perforation, inflammation or obstruction was observed during the study.

PDA probe preparation.

Barium sulfate particles (20 g) were added into Tris buffer (50 mM, 1000 ml at pH 8.5), followed by quick addition of dopamine (10 g). The reaction mixture was kept at room temperature with stirring (600 rpm) for 3 hours. The as-synthesized PDA probes were purified with centrifugation (4000 rpm x 10 min). The purified PDA probes were re-dispersed in 100 ml of water and sonicated. The purified PDA probes were lyophilized for 3 days and stored at −20 °C. Before administration, PDA probes were resuspended in the GSEL solution and the PDA-probe-GSEL solution was used fresh.

In vivo evaluation of intestinal retention of the PDA coating through X-ray imaging.

Pigs were sedated, intubated, and maintained with isoflurane as described above. The gastric fluid was removed from the stomach before administration. PDA probes (20 mg/ml) were first suspended in the GSEL solution. Pigs were orally administered the PDA-probe suspended GSEL solution (3 ml/kg), and introduced into the small intestine. Conventional radio-opaque probe (unmodified barium sulfate particles) suspended aqueous solution at the same concentration was administered as the control. Radiographs were performed to monitor the intestinal retention of the probes and PDA coating. For short-term stability evaluation, X-ray images were taken before and after rinsing the coated area with 500 ml of water. For long-term retention assessment, a series of X-ray images were periodically taken at designated time points in the same location, during which pigs consistently consumed a liquid diet. Additionally, pigs were assessed clinically and radiographically for evidence of gastrointestinal perforation and obstruction (*e.g.*, inappetence, abdominal distension, lack of stool, or vomiting). No clinical or radiographic evidence of gastrointestinal perforation and obstruction was observed during the study.

In vivo coating exogenous β-galactosidase on intestinal epithelium.

Pigs were anesthetized, intubated, and maintained with isoflurane as described above. The gastric fluid was removed from the stomach before administration. A laparotomy was performed on pigs to open up the small intestine. A chamber was placed on top of the

intestinal epithelium, followed by addition of the GSEL solution (3 ml) with suspended β-galactosidase (5 μg/ml). Three control chambers containing solutions with and without the key agents (β-galactosidase and GSEL solution) were also placed in the same pig. After 20 minutes of coating, epithelium inside the chamber was washed 3 times with water, and the β-gal activity of the tissue was evaluated by using o-nitrophenol-β-D-galactoside (ONPG) as substrate.

PDA nano-crosslinker preparation and characterization.

Ammonium hydroxide (10 ml, 28–30% w/w) was diluted into 650 ml ethanol-water (4:9 ratio v/v) mixed solution. The mixed solution was stirred under at 30 °C for 1 hour, followed by addition of 50 ml dopamine solution (50 mg/ml in water). The reaction mixture was kept at 30 °C for 24 hours. The as-synthesized PDA nano-crosslinkers were purified with centrifugation (6000 rpm x 15 min). The purified PDA nano-crosslinkers were re-dispersed in 500 ml of water and sonicated. The dry size and hydrodynamic size were measured with a transmission electron microscope (TEM, JEOL 2100F, JEOL. Ltd) and a Zetasizer Nano ZS90 instrument (Malvern Panalytical), respectively.

Ex vivo evaluation of blocking efficiency of the GSEL coating.

Tissues were exposed to the GSEL solution and washed with PBS buffer (1X) 3 times to remove excess PDA. PDA nano-crosslinkers with different concentrations (25 mg/ml, 12.5 mg/ml, and 0 mg/ml) were suspended in the GSEL solution. The coated tissues were placed in the Franz Cell, 100 mM nutrients ($CaCl_2$, glutamic acid and glucose) were added separately into the chamber (occluded with Parafilm), and the samples were taken from the receptor compartment (with stir bars) for measurements after 3 hours.

In vivo evolution of the impermeable PDA coating for preventing glucose uptake.

Pigs (fasted overnight) were sedated, intubated, and maintained with isoflurane as described above. The gastric fluid was removed from the stomach before administration. PDA nano-crosslinkers (25 mg/ml) were first suspended in the GSEL solution. Pigs were orally administered the nano-crosslinker suspended GSEL solution (10 ml/kg), and introduced into the small intestine. The solution was directly administered to the small intestine through a catheter under endoscopic visual guidance. For controls, 500 ml of water solution was administered in the same way. Standard oral glucose tolerance test (OGTT) tests were performed on pigs after 20 minutes of GSEL solution administration(6, 60). Pigs were orally administered the aqueous glucose solution (3 ml/kg, 500 mg/ml), and introduced into the small intestine. Blood samples were collected from a central venous line at designated time points, and immediately tested for glucose concentrations using a OneTouch Ultra glucose monitor (LifeScan Inc). Each data point (blood glucose change) was plotted with time, and area under the curve was calculated for quantitative evaluation.

Praziquantel-GSEL solution preparation.

Praziquantel particles were encapsulated in PDA, allowing the reactive groups (*e.g.* catechol and amine groups) on the PDA surface to enable chemical crosslinking and incorporation of praziquantel particles into the PDA coating layer. Additionally, the hydrophilic PDA layer

on the particle surface dramatically improves the stability and dispersion property of hydrophobic drug particles(61, 62). Praziquantel particles (powder) (8 g) were sieved (150–300 μm mesh size) and added into Tris buffer (50 mM, 400 ml at pH 8.5), followed by quick addition of dopamine (4 g)(63). The reaction mixture was kept at room temperature and stirred (600 rpm) for 3 hours. The as-synthesized praziquantel particles were purified with centrifugation (4000 rpm x 10 min). The purified praziquantel particles were lyophilized for 3 days and stored at −20 °C. Before administration, praziquantel particles were resuspended in the GSEL solution and the praziquantel-GSEL solution was used fresh.

Praziquantel concentration assessment.

High-Performance Liquid Chromatography Agilent 1260 Infinity II HPLC system (Agilent Technologies, Inc.) equipped with Model 1260 quaternary pump, Model 1260 Hip ALS autosampler, Model 1290 thermostat, Model 1260 TCC control module, and Model 1260 diode array detector was utilized as described previously. Data processing and analysis was performed using OpenLab CDS software (Agilent Technologies, Inc.). For praziquantel, chromatographic isocratic separation was carried out on an Agilent Zorbax Eclipse XDB C-18 4.6 × 150 mm analytical column with 5 μm particles, maintained at 40 °C. The optimized mobile phase consisted of MilliQ grade water and acetonitrile at a flow rate of 1 ml/min over a 5 minutes run time. Separation was achieved using a gradient elution profile starting at 50% water and 50% acetonitrile at minute 0 which ended at 30% water and 70% acetonitrile at 3 minutes. The injection volume was 5 μl, and the selected ultraviolet (UV) detection wavelength was 217 nm.

In vivo evolution of pharmacokinetics of the praziquantel-GSEL solution.

Pigs were sedated, intubated, and maintained with isoflurane as described above. The gastric fluid was removed from the stomach before administration. Praziquantel-GSEL solution (20 mg/ml, 1 ml/kg) was delivered into the small intestine. Praziquantel without the GSEL solution was used as the control. Blood samples were collected from a marginal ear vein at designated time points. Serum samples were separated from blood by centrifugation (1800 G x 10 min at 4 °C) and were stored at −80 °C for further analysis.

Oral toxicity test.

Three groups (4 animals in each group) of rats (Sprague Dawley, 150–200 g, Charles River Labs) were exposed to the water (5 ml/kg), as-prepared PDA (15 mg/ml, 5 ml/kg) and GSEL solution (5 ml/kg) separately over a period of 4 weeks by following guidelines issued by Organization for Economic Co-operation and Development (OECD) with minor modifications(55). The solution was directly administered to rats through gavage needles, but not endoscopic catheters. Body weights were measured every day for 28 days. Blood samples were collected at day 27 for hematological and blood biochemistry measurements. At day 28, all 12 rats were euthanized and a necropsy was performed. Samples of heart, lung, liver, kidney, spleen, stomach, small intestine, and large intestine were collected for histological analyses.

Histological analyses of tissues.

Tissues were first fixed in PBS buffer (1X) with 4% paraformaldehyde for 6 hours and then placed into PBS buffer with 30% sucrose overnight at 4 °C. The fixed tissues were embedded in paraffin and cut into 5-μm-thick sections with a cryostat (Leica Biosystems). The sections were stained with hematoxylin and eosin for histopathological analysis.

PDA coating of impermeable polycarbonate sheets.

Polycarbonate sheets were exposed to the GSEL solution (without H_2O_2) for 36 hours and washed with water to remove excess PDA.

Statistical analysis.

All data were reported as means ± SD for $n \geq 3$ measurements for each group. Two-sample *t* tests, one-way ANOVA, and post hoc Bonferroni multiple comparisons test were used to determine the significance. Individual subject-level data are provided in data file S1.

Supplementary Material

Refer to Web version on PubMed Central for supplementary material.

ACKNOWLEDGEMENTS:

We are grateful to R. S. Langer for invaluable guidance and comments on this work. A. R. Kirtane is thankful to PhRMA foundation postdoctoral fellowship. We are grateful to all members of the Langer and Traverso Laboratories, especially M. Verma, T. V. Erlach, S. Babaee, J. Coffey, J. Li, H. Mazdiyasni, R. Xiao, J. Byrne, X. Lu, and C. Steiger for discussion of mechanisms and applications of GSEL. We are also grateful to E. Caffarel-Salvador, V. Soares and M. Jimenez for help with human tissue and bacteria samples.

Funding: This work was supported in part by the Bill and Melinda Gates Foundation Grants (OPP1179091), NIH (EB000244) and funds from the Department of Mechanical Engineering, MIT.

REFERENCES

1. Turner JR, Intestinal mucosal barrier function in health and disease, Nat. Rev. Immunol. 9, 799–809 (2009). [PubMed: 19855405]
2. Peterson LW, Artis D, Intestinal epithelial cells: regulators of barrier function and immune homeostasis, Nat. Rev. Immunol. 14, 141–153 (2014). [PubMed: 24566914]
3. Anselmo AC, Gokarn Y, Mitragotri S, Non-invasive delivery strategies for biologics, Nat. Rev. Drug Discov. 18, 19–40 (2018). [PubMed: 30498202]
4. Zelikin AN, Ehrhardt C, Healy AM, Materials and methods for delivery of biological drugs, Nat. Chem. 8, 997–1007 (2016). [PubMed: 27768097]
5. Mohanaruban A, Patel N, Ashrafian H, Stoenchev K, Le Roux C, Penney N, Kelly J, Byrne J, Hopkins J, Mason J, Teare J, PTH-003 Endobarrier®: a safe and effective novel treatment for obesity and type 2 diabetes?, Endoscopy 66, A205.1-A205 (2017).
6. Lee Y, Deelman TE, Chen K, Lin DSY, Tavakkoli A, Karp JM, Therapeutic luminal coating of the intestine, Nat. Mater. 17, 834–842 (2018). [PubMed: 29891893]
7. Kitano K, Schwartz DM, Zhou H, Gilpin SE, Wojtkiewicz GR, Ren X, Sommer CA, Capilla AV, Mathisen DJ, Goldstein AM, Mostoslavsky G, Ott HC, Bioengineering of functional human induced pluripotent stem cell-derived intestinal grafts, Nat. Commun. 8, 765 (2017). [PubMed: 29018244]
8. Rajagopalan H, Cherrington AD, Thompson CC, Kaplan LM, Rubino F, Mingrone G, Becerra P, Rodriguez P, Vignolo P, Caplan J, Rodriguez L, Galvao Neto MP, Endoscopic duodenal mucosal

resurfacing for the treatment of type 2 diabetes: 6-month interim analysis from the first-in-human proof-of-concept study., Diabetes Care 39, 2254–2261 (2016). [PubMed: 27519448]

9. Kaukinen K, Lindfors K, Mäki M, Advances in the treatment of coeliac disease: an immunopathogenic perspective, Nat. Rev. Gastroenterol. Hepatol. 11, 36–44 (2014). [PubMed: 23917697]
10. Torres J, Mehandru S, Colombel J-F, Peyrin-Biroulet L, Crohn's disease, Lancet 389, 1741–1755 (2017). [PubMed: 27914655]
11. Green PHR, Cellier C, Celiac disease, N. Engl. J. Med 357, 1731–1743 (2007). [PubMed: 17960014]
12. Camaschella C, Iron-deficiency anemia, N. Engl. J. Med. 372, 1832–1843 (2015). [PubMed: 25946282]
13. Yui S, Nakamura T, Sato T, Nemoto Y, Mizutani T, Zheng X, Ichinose S, Nagaishi T, Okamoto R, Tsuchiya K, Clevers H, Watanabe M, Functional engraftment of colon epithelium expanded in vitro from a single adult Lgr5+ stem cell, Nat. Med. 18, 618–623 (2012). [PubMed: 22406745]
14. Elloumi-Hannachi I, Yamato M, Okano T, Cell sheet engineering: a unique nanotechnology for scaffold-free tissue reconstruction with clinical applications in regenerative medicine, J. Intern. Med. 267, 54–70 (2010). [PubMed: 20059644]
15. Kirkegaard P, Christensen AB, Ibsen J, Hegedüs V, Christiansen J, Experimental nonsuture colonic anastomoses, Am. J. Surg. 139, 233–236 (1980). [PubMed: 7356107]
16. Fishbein TM, Intestinal transplantation, N. Engl. J. Med 361, 998–1008 (2009). [PubMed: 19726774]
17. Khademhosseini A, Langer R, A decade of progress in tissue engineering, Nat. Protoc. 11, 1775–1781 (2016). [PubMed: 27583639]
18. Odenwald MA, Turner JR, The intestinal epithelial barrier: a therapeutic target?, Nat. Rev. Gastroenterol. Hepatol. 14, 9–21 (2017). [PubMed: 27848962]
19. Carino GP, Mathiowitz E, Oral insulin delivery, Adv. Drug Deliv. Rev. 35, 249–257 (1999). [PubMed: 10837700]
20. Thakral S, Thakral NK, Majumdar DK, Eudragit®: a technology evaluation, Expert Opin. Drug Deliv. 10, 131–149 (2013). [PubMed: 23102011]
21. Khan MZI, Prebeg Ž, Kurjaković N, A pH-dependent colon targeted oral drug delivery system using methacrylic acid copolymers. I. Manipulation of drug release using Eudragit® L100–55 and Eudragit® S100 combinations, J. Control. Release 58, 215–222 (1999). [PubMed: 10053194]
22. Laulicht B, Tripathi A, Mathiowitz E, Diuretic bioactivity optimization of furosemide in rats, Eur. J. Pharm. Biopharm. 79, 314–319 (2011). [PubMed: 21571067]
23. Abramson A, Caffarel-Salvador E, Soares V, Minahan D, Tian RY, Lu X, Dellal D, Gao Y, Kim S, Wainer J, Collins J, Tamang S, Hayward A, Yoshitake T, Lee HC, Fujimoto J, Fels J, Frederiksen MR, Rahbek U, Roxhed N, Langer R, Traverso G, A luminal unfolding microneedle injector for oral delivery of macromolecules, Nat. Med. 25, 1512–1518 (2019). [PubMed: 31591601]
24. Harris FC, Pyloric stenosis: hold-up of enteric coated aspirin tablets, Br. J. Surg. 60, 979–981 (1973). [PubMed: 4764749]
25. Abuhelwa AY, Foster DJR, Upton RN, A quantitative review and meta-models of the variability and factors affecting oral drug absorption—part I: gastrointestinal pH, AAPS J. 18, 1309–1321 (2016). [PubMed: 27495120]
26. Dressman J, Krämer J, Pharmaceutical dissolution testing (Taylor & Francis, 2005).
27. Lee H, Dellatore SM, Miller WM, Messersmith PB, Mussel-inspired surface chemistry for multifunctional coatings., Science 318, 426–30 (2007). [PubMed: 17947576]
28. Lee H, Rho J, Messersmith PB, Facile conjugation of biomolecules onto surfaces via mussel adhesive protein inspired coatings, Adv. Mater. 21, 431–434 (2009). [PubMed: 19802352]
29. U.S. Food and Drug Administration, Oral health care drug products for over-the-counter human use; antigingivitis/antiplaque drug products; establishment of a monograph; proposed rules, Fed. Regist. 68, 32232–32287 (2003).
30. Ofikwu GI, Sarhan M, Ahmed L, EVICEL glue-induced small bowel obstruction after laparoscopic gastric bypass., Surg. Laparosc. Endosc. Percutan. Tech. 23, e38–40 (2013). [PubMed: 23386172]

31. Fagerberg L, Hallström BM, Oksvold P, Kampf C, Djureinovic D, Odeberg J, Habuka M, Tahmasebpoor S, Danielsson A, Edlund K, Asplund A, Sjöstedt E, Lundberg E, Szigyarto CA-K, Skogs M, Takanen JO, Berling H, Tegel H, Mulder J, Nilsson P, Schwenk JM, Lindskog C, Danielsson F, Mardinoglu A, Åsa Sivertsson K. von Feilitzen M. Forsberg M. Zwahlen I. Olsson S. Navani M. Huss J. Nielsen F. Ponten M. Uhlén, Analysis of the human tissue-specific expression by genome-wide integration of transcriptomics and antibody-based proteomics, Mol. Cell. Proteomics 13, 397 (2014).
32. Lomer MCE, Parkes GC, Sanderson JD, Review article: lactose intolerance in clinical practice-myths and realities, Aliment. Pharmacol. Ther. 27, 93–103 (2007). [PubMed: 17956597]
33. Storhaug CL, Fosse SK, Fadnes LT, Country, regional, and global estimates for lactose malabsorption in adults: a systematic review and meta-analysis, Lancet Gastroenterol. Hepatol. 2, 738–746 (2017). [PubMed: 28690131]
34. Rosado JL, Solomons NW, Lisker R, Bourges H, Anrubio G, García A, Perez-Briceño R, Aizupuru E, Enzyme replacement therapy for primary adult lactase deficiency: effective reduction of lactose malabsorption and milk intolerance by direct addition of β-galactosidase to milk at mealtime, Gastroenterology 87, 1072–1082 (1984). [PubMed: 6434367]
35. Leader B, Baca QJ, Golan DE, Protein therapeutics: a summary and pharmacological classification, Nat. Rev. Drug Discov. 7, 21–39 (2008). [PubMed: 18097458]
36. American Diabetes Association, 2. Classification and diagnosis of diabetes: standards of medical care in diabetes-2018, Diabetes Care 41, S13–S27 (2018). [PubMed: 29222373]
37. Mingrone G, Panunzi S, De Gaetano A, Guidone C, Iaconelli A, Leccesi L, Nanni G, Pomp A, Castagneto M, Ghirlanda G, Rubino F, Bariatric surgery versus conventional medical therapy for type 2 diabetes, N. Engl. J. Med. 366, 1577–1585 (2012). [PubMed: 22449317]
38. Lin Z, Forster J, Sarosiek I, McCallum RW, Treatment of diabetic gastroparesis by high-frequency gastric electrical stimulation, Diabetes Care 27, 1071–1076 (2004). [PubMed: 15111523]
39. Bellinger AM, Jafari M, Grant TM, Zhang S, Slater HC, Wenger EA, Mo S, Lee Y-AL, Mazdiyasni H, Kogan L, Barman R, Cleveland C, Booth L, Bensel T, Minahan D, Hurowitz HM, Tai T, Daily J, Nikolic B, Wood L, Eckhoff PA, Langer R, Traverso G, Oral, ultra-long-lasting drug delivery: application toward malaria elimination goals., Sci. Transl. Med 8, 365ra157 (2016).
40. Liu J, Pang Y, Zhang S, Cleveland C, Yin X, Booth L, Lin J, Lucy Lee Y-A, Mazdiyasni H, Saxton S, Kirtane AR, von Erlach T, Rogner J, Langer R, Traverso G, Triggerable tough hydrogels for gastric resident dosage forms, Nat. Commun. 8, 124 (2017). [PubMed: 28743858]
41. Doenhoff MJ, Cioli D, Utzinger J, Praziquantel: mechanisms of action, resistance and new derivatives for schistosomiasis, Curr. Opin. Infect. Dis. 21, 659–667 (2008). [PubMed: 18978535]
42. Vale N, Gouveia MJ, Rinaldi G, Brindley PJ, Gärtner F, Correia da Costa JM, Praziquantel for schistosomiasis: single-drug metabolism revisited, mode of action, and resistance., Antimicrob. Agents Chemother. 61, e02582–16 (2017).
43. Tokura Y, Harvey S, Chen C, Wu Y, Ng DYW, Weil T, Fabrication of defined polydopamine nanostructures by DNA origami-templated polymerization, Angew. Chemie Int. Ed. 57, 1587–1591 (2018).
44. Bisaglia M, Mammi S, Bubacco L, Kinetic and structural analysis of the early oxidation products of dopamine: analysis of the interactions with α-synuclein, J. Biol. Chem. 282, 15597–15605 (2007).
45. Traverso G, Langer R, Perspective: special delivery for the gut, Nature 519, S19–S19 (2015). [PubMed: 25806494]
46. Li J, Baird MA, Davis MA, Tai W, Zweifel LS, Waldorf KMA, Gale M Jr, Rajagopal L, Pierce RH, Gao X, Dramatic enhancement of the detection limits of bioassays via ultrafast deposition of polydopamine, Nat. Biomed. Eng. 1, 0082 (2017).
47. Connock M, Pover W, Catalase particles in the epithelial cells of the guinea-pig small intestine, Histochem. J. 2, 371–380 (1970). [PubMed: 5525787]
48. Winterwerber P, Harvey S, Ng DYW, Weil T, Photocontrolled dopamine polymerization on DNA origami with nanometer resolution, Angew. Chemie Int. Ed. 59, 6144–6149 (2020).

49. Ball V, Del Frari D, Toniazzo V, Ruch D, Kinetics of polydopamine film deposition as a function of pH and dopamine concentration: Insights in the polydopamine deposition mechanism, J. Colloid Interface Sci. 386, 366–372 (2012). [PubMed: 22874639]
50. Holmes JC, Fowler NO, Direct cardiac effects of dopamine, Circ. Res. 10, 68–72 (1962). [PubMed: 13908517]
51. Barker N, Adult intestinal stem cells: critical drivers of epithelial homeostasis and regeneration, Nat. Rev. Mol. Cell Biol. 15, 19–33 (2014). [PubMed: 24326621]
52. Hong S, Wang Y, Park SY, Lee H, Progressive fuzzy cation-assembly of biological catecholamines, Sci. Adv. 4, eaat7457 (2018).
53. Ponzio F, Le Houerou V, Zafeiratos S, Gauthier C, Garnier T, Jierry L, Ball V, Robust alginate-catechol@polydopamine free-standing membranes obtained from the water/air interface, Langmuir 33, 2420–2426 (2017). [PubMed: 28198631]
54. Thelen K, Dressman JB, Cytochrome P450-mediated metabolism in the human gut wall, J. Pharm. Pharmacol. 61, 541–558 (2009). [PubMed: 19405992]
55. OECD, Test no. 407: repeated dose 28-day oral toxicity study in rodentsOECD Guidel. Test. Chem. Sect. 4, OECD Publ. Paris, 1–10 (2008).
56. Kirkman HN, Gaetani GF, Mammalian catalase: a venerable enzyme with new mysteries, Trends Biochem. Sci. 32, 44–50 (2007). [PubMed: 17158050]
57. Heber D, Greenway FL, Kaplan LM, Livingston E, Salvador J, Still C, Endocrine and nutritional management of the post-bariatric surgery patient: An endocrine society clinical practice guideline, J. Clin. Endocrinol. Metab. 95, 4823–4843 (2010). [PubMed: 21051578]
58. Kirtane AR, Hua T, Hayward A, Bajpayee A, Wahane A, Lopes A, Bensel T, Ma L, Stanczyk FZ, Brooks S, Gwynne D, Wainer J, Collins J, Tamang SM, Langer R, Traverso G, A once-a-month oral contraceptive, Sci. Transl. Med. 11, eaay2602 (2019).
59. Babaee S, Pajovic S, Kirtane AR, Shi J, Caffarel-Salvador E, Hess K, Collins JE, Tamang S, Wahane AV, Hayward AM, Mazdiyasni H, Langer R, Traverso G, Temperature-responsive biometamaterials for gastrointestinal applications, Sci. Transl. Med. 11, eaau8581 (2019).
60. Manell E, Hedenqvist P, Svensson A, Jensen-Waern M, Xu E, Ed. Establishment of a refined oral glucose tolerance test in pigs, and assessment of insulin, glucagon and glucagon-like peptide-1 responses, PLoS One 11, e0148896 (2016).
61. Zhan H, Jagtiani T, Liang JF, A new targeted delivery approach by functionalizing drug nanocrystals through polydopamine coating, Eur. J. Pharm. Biopharm. 114, 221–229 (2017). [PubMed: 28161549]
62. Cui J, Wang Y, Postma A, Hao J, Hosta-Rigau L, Caruso F, Monodisperse polymer capsules: tailoring size, shell thickness, and hydrophobic cargo loading via emulsion templating, Adv. Funct. Mater. 20, 1625–1631 (2010).
63. Park J, Brust TF, Lee HJ, Lee SC, Watts VJ, Yeo Y, Polydopamine-based simple and versatile surface modification of polymeric nano drug carriers, ACS Nano 8, 3347–3356 (2014). [PubMed: 24628245]
64. Margoliash E, Margoliash A, A study of the inhibition of catalase by 3-amino-1:2:4:-triazole, Biochem. J. 68, 468–475 (1958). [PubMed: 13522646]

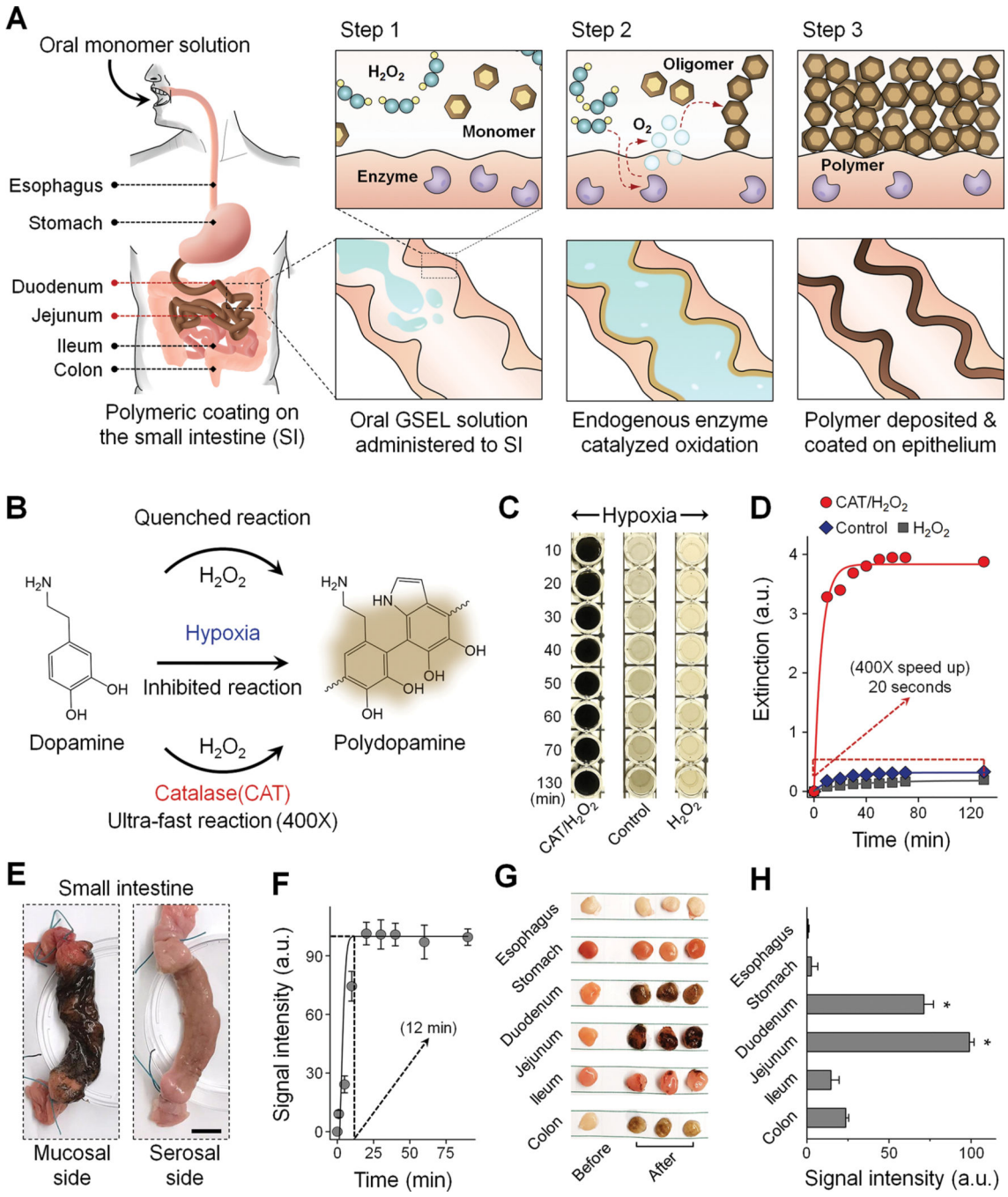

Fig. 1. Endogenous enzyme catalyzed PDA growth on small intestinal epithelium.

(**A**) Schematic illustration of the GSEL technology. Orally administered dopamine monomers in the GSEL solution rapidly oxidize in the presence of hydrogen peroxide (H_2O_2) under endogenous CAT catalysis, and form PDA coating on small intestinal epithelium. Specific small intestine coating and targeting is achieved due to the uneven distribution of CAT along the digestive tract (high expression in the small intestine). (**B**) Schematic illustration of the CAT-accelerated PDA polymerization in a hypoxic environment. In an oxygen-deficient environment, dopamine (colorless) oxidation (O_2 as

oxidant) and PDA (dark-brown color) formation are inhibited and almost quenched in the presence of H_2O_2. CAT can boost oxygen release (H_2O_2 as O_2 source) and accelerate PDA polymerization by about 400 times. (**C**) Visual observation of PDA polymerization under conditions shown in (**B**) at various time points. (**D**) Extinction measured at 700 nm for the samples in (**C**). The optical extinction produced in 20 seconds under CAT catalysis was the same as the extinction produced in 2 hours under other conditions. (**E**) Images showing PDA coating on the mucosal and serosal side of the porcine small intestine after same ex vivo coating treatment using the GSEL solution. Scale bar, 2 cm. (**F**) Quantitative evaluation of the ex vivo GSEL coating kinetics. The PDA signal reached completion within 12 minutes. Data are reported as means ± SD over three porcine tissue samples. (**G**) Images showing porcine tissue samples from different parts of the GI tract before and after the ex vivo GSEL coating. Samples (6 mm in diameter) were collected at three random sites from PDA-coated tissue. (**H**) Quantitative measurements of the PDA signal intensities of samples shown in (**G**). The intensity differences between the small intestine and other tissues are statistically significant. $*P < 0.05$, one-way analysis of variance (ANOVA) and post hoc Bonferroni. Data are reported as means ± SD over over three different tissue samples.

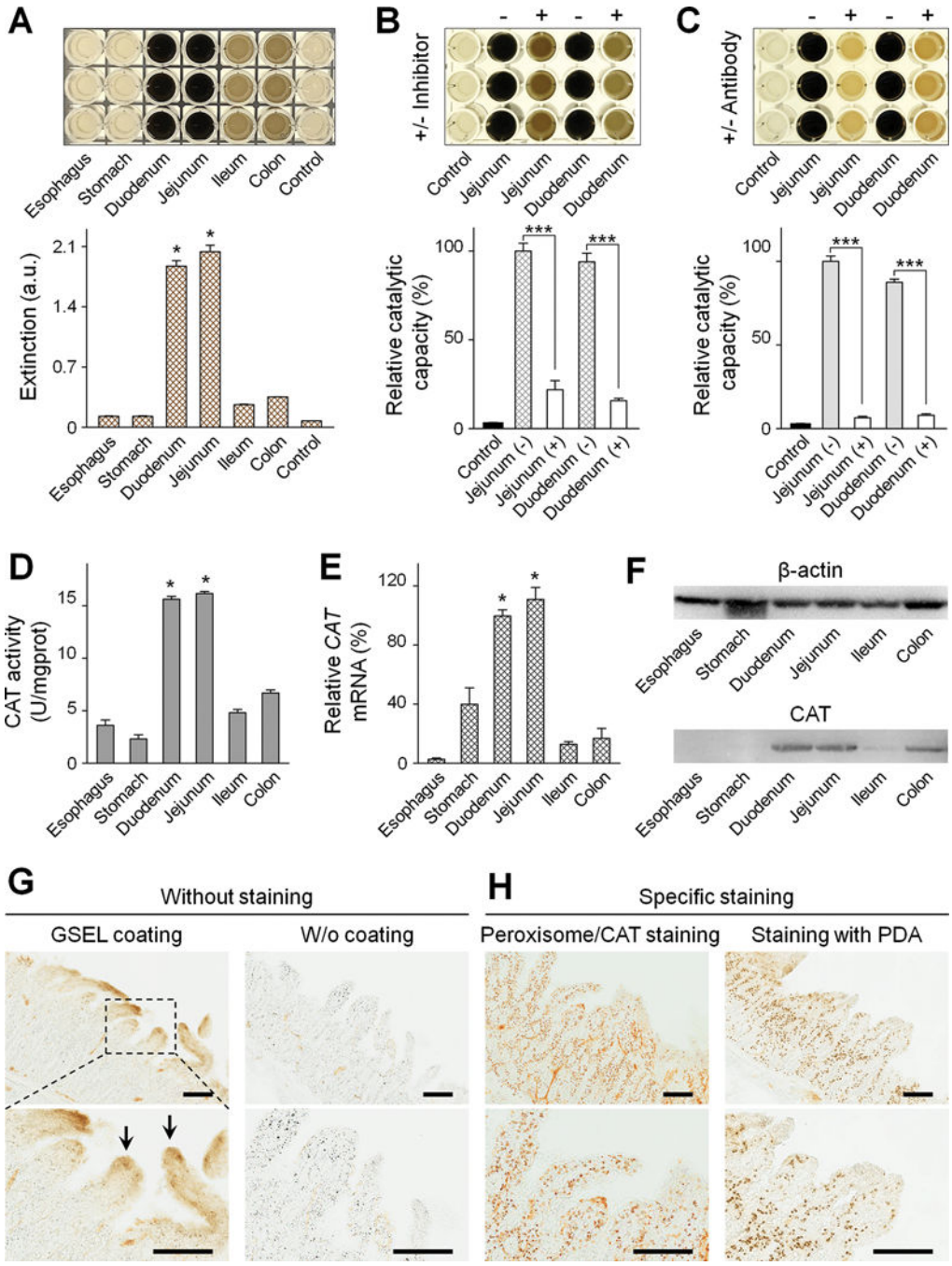

Fig. 2. Biological mechanisms of GSEL.

(**A**) Evaluation of the relationship between tissue catalytic capacity and PDA polymerization. Porcine tissue lysates were added individually into the GSEL solution, and the extinction of each solution was measured at 700 nm. Top panel: visual assessments; bottom panel: quantitative measurements. Small intestinal epithelium was significantly different from other tissues and control (without lysates). *P < 0.05, one-way ANOVA and post hoc Bonferroni. Data are reported as means ± SD over three replicates. (**B & C**) Verification of the exclusive role of CAT in reactions shown in (**A**) by treating the lysates

with either a (**B**) CAT-specific inhibitor or (**C**) antibody that induces immunoprecipitation. The relative catalytic capacity differences between the treated and untreated groups are statistically significant. ***$P < 0.001$ by two-tailed *t*-test. Data are reported as means ± SD over three different tissue samples. (**D**-**F**) Quantification of CAT expression (gene and protein) along the porcine GI tract by (**D**) CAT activity analysis, (**E**) real-time PCR, and (**F**) western blotting. Similar distribution profiles were achieved in (**D**-**F**), indicating significantly higher CAT expression in the small intestinal epithelium compared to other tissues. *$P < 0.05$, one-way ANOVA and post hoc Bonferroni. Data are reported as means ± SD over three replicates. (**G**) Microscopic analysis of PDA-coated porcine small intestinal epithelium, showing a thin PDA layer coated on the exterior villi (indicated by arrows), but nothing on control tissue (without coating). Scale bars, 150 μm. (**H**) Bright-field imaging of uncoated tissue slices treated by specific peroxisome/CAT staining (left panels) and with the GSEL solution (right panels). Scale bars, 150 μm.

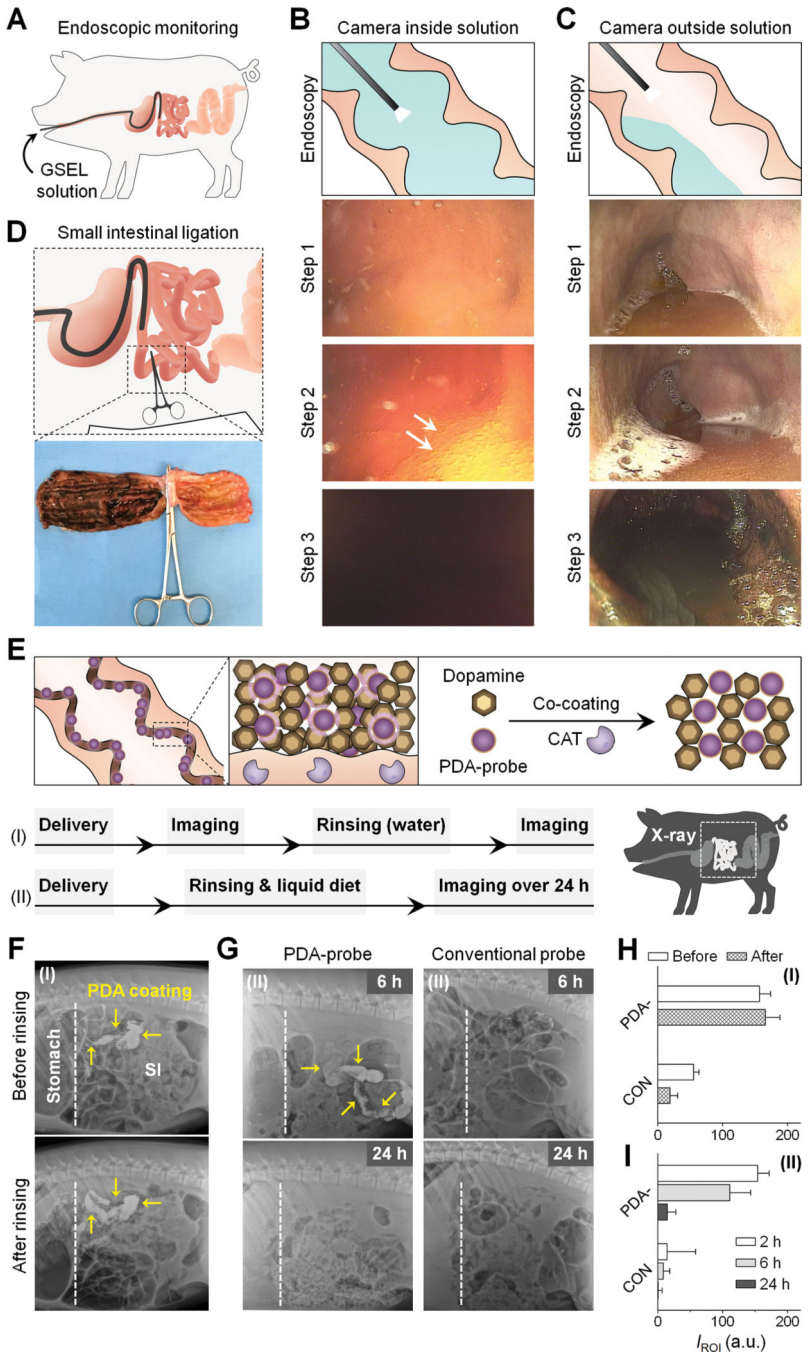

Fig. 3. In vivo performance of the GSEL coating in pigs.

(**A-C**) Schematics and photographs of in vivo GI endoscopic real-time recording of PDA formation during the GSEL process. The GSEL solution was directly administered to the porcine small intestine through a catheter under endoscopic visual guidance, and the endoscopic camera was placed both inside and outside the solution within the small intestine for observation. (**B & C**) Endoscopic images (bottom three panels) revealing the steps during PDA coating. Oxygen bubbles were generated at the epithelium-solution interface (indicated by white arrows). (**D**) Schematic illustration of porcine small intestinal ligation

(top panel) and photograph of direct PDA coating evaluation (bottom panel). The GSEL solution filled the intestinal cavity up until the clamp site, unable to pass down to the lower small intestine. (**E**) Schematic illustration of intestinal retention of the PDA coating indicated by X-ray imaging of the PDA probes. X-ray images were taken for two in vivo tests: (I) short-term stability evaluation (rinsing the coated area) and (II) long-term retention assessment (liquid diet for 24 hours). (**F**) X-ray images of PDA probes as well as the PDA coating layer stably residing in the porcine small intestine before and after rinsing the imaging area, shown in test (I). The stomach and small intestine (SI) areas were separated with white dotted lines. PDA coating is indicated by yellow arrows. (**G**) X-ray images of intestinal retention of PDA coating for the duration of test (II). Conventional probes were nearly undetectable after food exposure. (**H**) Quantitative signal intensity analysis of coated small intestine areas, regions of interest (ROI), in (**F**). Data are reported as means ± SD over three different measurements. (**I**) Quantitative signal intensity analysis of the PDA coating over time in (**G**). Data are reported as means ± SD over three different measurements.

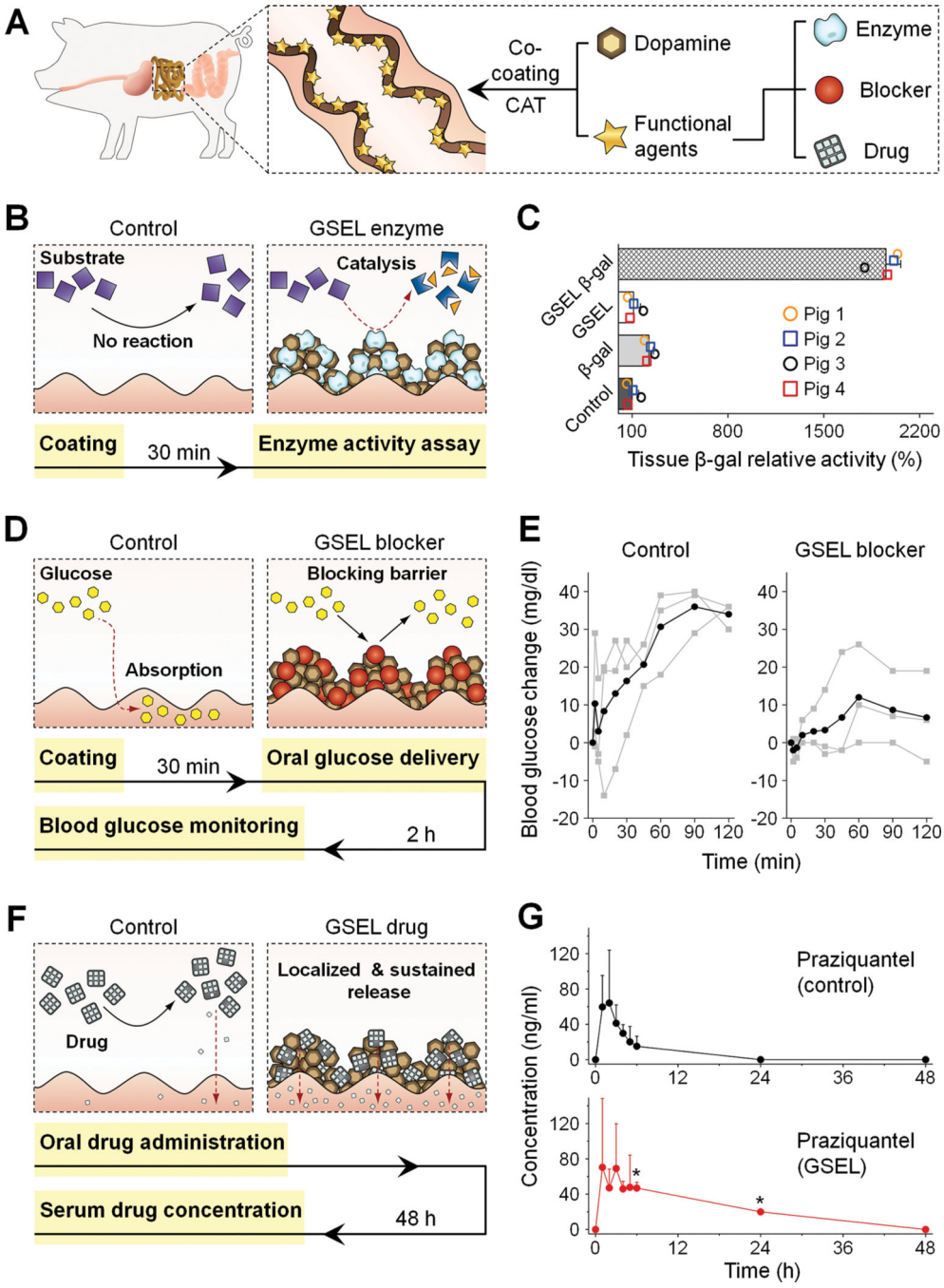

Fig. 4. Therapeutic applications enabled by GSEL.

(**A**) Schematic illustration of the GSEL therapeutic platform. Functional agents, including a digestive enzyme, nutrient blocker, and anthelmintic drug, were incorporated into the platform through co-administering with the GSEL orally to pigs. (**B**) Schematic illustration of incorporating digestive enzymes (β-galactosidase, β-gal) into PDA coating layer on porcine intestinal epithelium for augmenting the digestion of substrates (lactose). After the in vivo coating, the β-gal activity of the coated epithelium was evaluated. (**C**) Quantitative comparison of β-gal activity showing increased enzymatic activity in GSEL-based β-gal

coated tissues compared to negative controls. Data are reported as means ± SD over four animals. (**D**) Schematic illustration of incorporating nano-crosslinkers (blockers) into the GSEL coating to enable an impermeable PDA coating layer, preventing glucose uptake in the porcine small intestine. After the in vivo coating, oral glucose was administered to the pigs, followed by monitoring blood glucose concentrations. (**E**) Quantitative comparison of blood glucose changes showing reduced blood glucose responses of the pigs with the GSEL coating relative to the control (without coating). Data was averaged between animals (each animal represented by a grey line) in each group (shown by the black line). (**F**) Schematic illustration of coating drug (praziquantel) particles on porcine intestinal epithelium for sustained release of therapeutics in the small intestine. After the in vivo oral administration of the praziquantel-GSEL solution, serum drug concentrations were analyzed over 48 hours. (**G**) Quantitative comparison of the pharmacokinetics showing significantly extended retention time of the praziquantel (with the GSEL solution) relative to the control (without GSEL solution). *indicates $p < 0.02$, two sample t test comparing praziquantel-GSEL and control groups at matching time points. Data are reported as means ± SD over three animals.

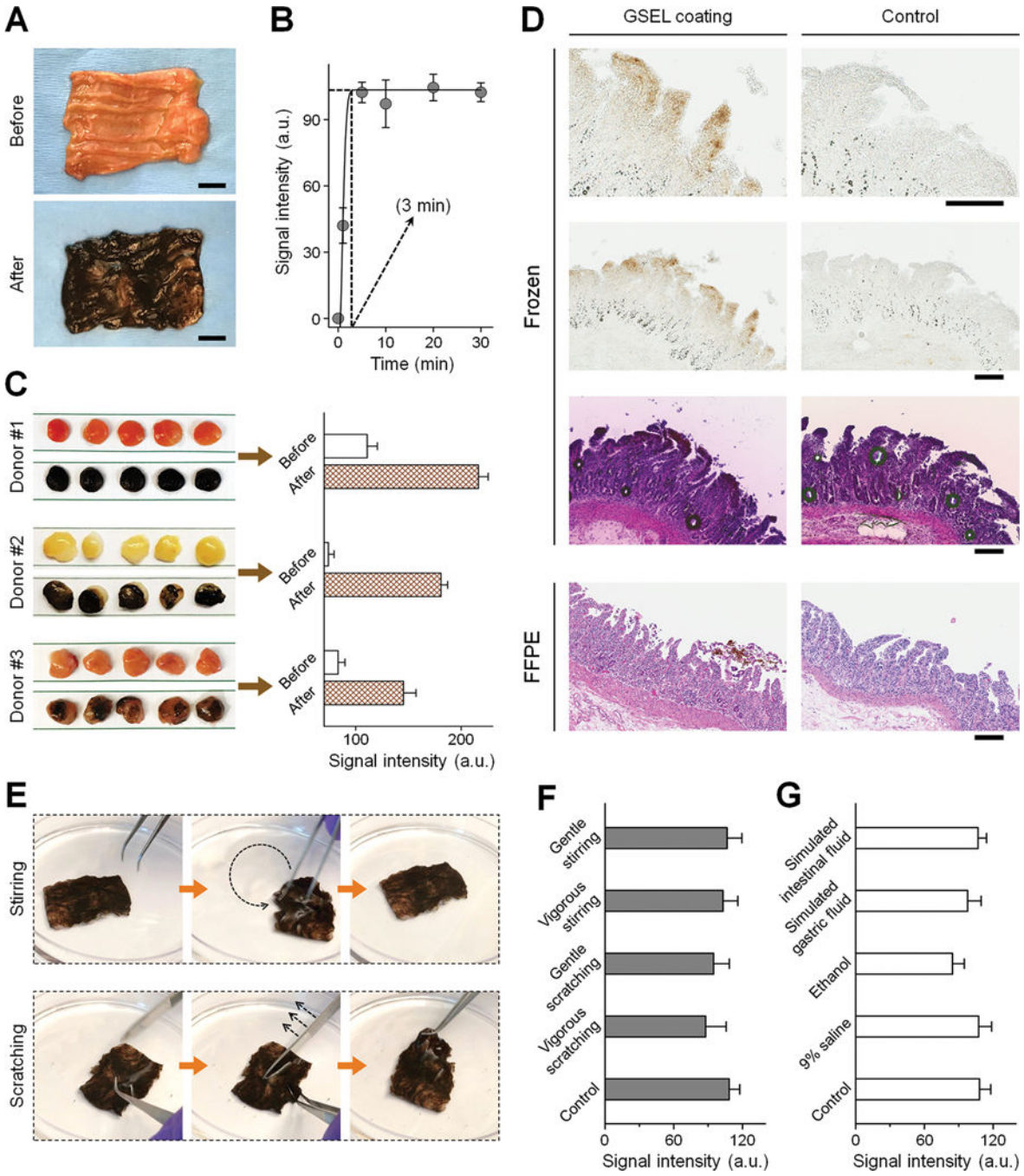

Fig. 5. Compatibility of human tissues with GSEL.

(**A**) Images showing fresh resected tissue specimens from human small intestine before and after ex vivo GSEL coating. Scale bar, 1 cm. (**B**) Coating kinetics showing ultrafast PDA signal development in human tissues ex vivo. The PDA signal reaches completion within 3 minutes. (**C**) Evaluation of GSEL consistency. Tissue specimens from 3 donors with different ages, races and genders were tested. Five ex vivo assessments were performed on random sites of the human small intestine. Quantitative measurements (right panel) of the PDA coating signals of samples (6 mm diameter) before and after coating (left panels)

confirmed consistent GSEL coating performance. Data are reported as means ± SD over five replicates. (**D**) Microscopic and histological analyses of frozen specimens (40 μm thickness) and FFPE specimens (5 μm thickness) collected from PDA-coated human small intestinal epithelium. A thin PDA layer was observed on the exterior villi of coated tissues. Uncoated tissues were used as controls. Histological study [hematoxylin and eosin (H&E) staining] of adjacent frozen tissue slides and FFPE samples showed that the epithelial layers remained intact, with staining patterns similar to controls, demonstrating the absence of tissue toxicity. Scale bars, 150 μm. (**E**) Representative images from movie S1 showing no obvious PDA signal reduction in coated human small intestine after ex vivo mechanical stirring and scratching. (**F**) Quantitative ex vivo evaluation of PDA signal intensities of coated human tissues under a series of physical conditions. The intensity differences among all conditions are not statistically significant (two-tailed *t*-test). Data are reported as means ± SD over three replicates. (**G**) Quantitative ex vivo evaluation of PDA signal intensities of coated human tissues under a series of chemical conditions. The intensity differences among all conditions are not statistically significant (two-tailed *t*-test). Data are reported as means ± SD over three replicates.